Module 5: Schlieren and Shadowgraph

Lecture 32: Results and discussion related to crystal growth (part 2)

The Lecture Contains:

Convection Phenomena During Crystal Growth

- Effect of Crystal Size
- Competing Mechanisims in Concvection
- Tomographic Reconstruction of Schlieren Data
- Convection Around a Growing KDP Crystal
- Growth Patterns in the Diffusion Regime

Previous Next

EFFECT OF CRYSTAL SIZE

In the previous sections, it is seen that the crystal growth rate is positively correlated with the local concentration gradients. The gradients in turn depend on the size of the crystal, ramp rate and the rate of rotation. It is of interest to know if the gradients are explicit functions of time. An absence of time-dependence would show the process to be quasi-steady, and the results obtained in the present work would be applicable with greater generality.

To test the experimental data for the presence of growth history and inertia effects, the following experiments were performed: Previously grown crystals of small, medium and large sizes were suddenly inserted into the supersaturated solution. The solution was subjected to cooling at the prescribed ramp rate (of $0.1°C/hour$). The short time convection currents around a passive crystal have been compared with those that evolve gradually around a growing one when the growth process takes place from a seed, for a longer duration of time (~ 60-70 hours). A favorable comparison in terms of convection patterns is an indicator that the concentration gradients respond directly to the process parameters, and are not explicit functions of evolutionary time.

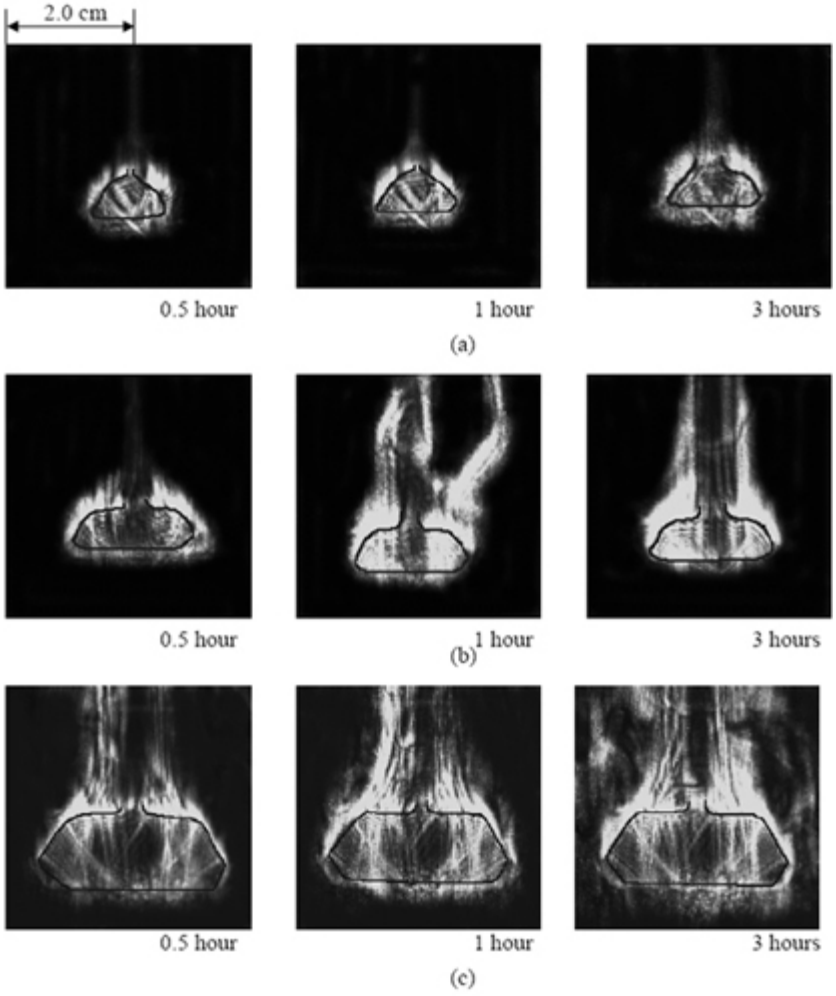

Figure 5.25: Schlieren images showing the instantaneous evolution of buoyancy-driven convection currents in the growth chamber when a crystal of (a) small, (b) medium and (c) large size is inserted into its supersaturated solution.

Previous Next

Figure 5.25 shows instantaneous schlieren images of buoyancy-driven convection around the crystal of varying sizes (small, medium and large) over a duration of 3 hours. Compared to the time durations generally required, this is a small time scale. Figure 5.25 shows that short time transients are indeed present in the solution, but they decay within a time frame of three hours for the three sizes considered. Over this time frame, the change in the crystal size was found to be negligible. Figure 5.25 shows that the strength of convection is weaker during the transient phase, and is the most vigorous when steady state appropriate for the size of the crystal is reached. The convection plumes during the transient phase can be unsteady and unsymmetrical. The loss of symmetry is related to the imperfections in the initial crystal geometry. The unsymmetrical plume is responsible for inducing flow unsteadiness above the crystal. With the passage of time, minor imperfections of the crystal are accommodated and the plume becomes symmetric as well as steady. The schlieren images in Figure 5.25 recorded at the end of 3 hours of experimentation correlate well with those shown in Figure 5.23 (Lecture 31). The similarity of buoyant plumes in the two configurations reveals that the long-time crystal growth process is indeed quasi-steady. Figure 5.25 also shows that departure from quasi-steady growth conditions can result in loss of symmetry and unsteady plume movement, both of which are undesirable from the view-point of crystal quality.

Previous Next

COMPETING MECHANSIMS IN CONVECTION

The relative importance of buoyant convection over rotation is discussed in the present section in fundamental terms. Essentially, the increase in crystal size takes place owing to the deposition of excess salt in the solution on the crystal faces. The speed at which the deposition occurs is proportional to the gradients in solutal concentration prevailing in this region. The gradients in turn depend on the pattern of fluid motion in the crystal growth chamber. The influence of fluid motion on concentration gradients can be explained in terms of solutal boundary-layers (*diffusion boundary-layers*) adjacent to the crystal faces. The boundary-layer thickness decreases as the fluid velocity increases. Clearly vigorous convective motion will increase concentration gradients, ultimately leading to a rapid increase in crystal size.

The conditions under which flow is intensified can be understood in terms of the forces acting on the fluid particles. For the solution contained in the beaker, the external force arises from buoyancy (in a gravitational field), while inertia forces related to linear and rotational acceleration are also present. The motion, in all situations is retarded by fluid viscosity. The forces are conveniently explained in terms of the dimensionless parameters Ra, the Rayleigh number and Re, the Reynolds number. Rayleigh number denotes the ratio of energy available in a buoyancy field and energy required to overcome viscous forces. Reynolds number is a ratio of rotational and viscous forces.

$$Ra = g\beta\Delta C L^3/v\alpha \qquad\qquad Re = \omega L^2/v$$

Here, g is acceleration due to gravity and β is the volumetric expansion coefficient of the solution with respect to salt concentration $(= 0.1\ per\ mol)$. Further ΔC is the concentration difference between the saturated $(density\ 1.1717\ gm/cm^3)$ and super-saturated solution, L the crystal thickness in the vertical direction, v the kinematic viscosity $(= 1.073 \times 10^{-6}\ m^2/s)$ and α the mass diffusivity $(1.0 \times 10^{-9}\ m^2/s)$. The symbol ω is the crystal rotational speed. In the present set of experiments, the linear dimension L increases with time, till the excess solute in the vicinity of the crystal is fully utilized.

Previous Next

The relative importance of the Rayleigh and Reynolds numbers is defined by the ratio $A=Ra/Re^2$, often called the Archimedes number. When the parameter is far away from unity, Ra (for A>>1) or Re (for A<<1) alone will control the flow. For the ratio A close to unity, one can expect an interaction between the buoyant and rotational force fields. It is reasonable to expect that the critical value of the Archimedes number that defines transition from buoyancy to rotation-controlled flow regimes is geometry dependent. Two and three-dimensional geometries are expected to yield different critical values. In the absence of definite information, A=1 is used in the following discussion as a critical value.

For the experiments conducted in the present work, the Rayleigh number based on the smallest crystal diameter is 10^4, while based on the largest crystal diameter it is in excess of 10^6. The corresponding Reynolds numbers range from 0 (no rotation) to 8 (smallest crystal) to 110 (largest crystal). These changes occur primarily because of an increase in the crystal size, but also due to an increase in the concentration difference available in a higher ramp rate experiment. For a small rotating crystal, one can calculate the ratio A=156, while for a large rotating crystal, A=82. Clearly, A>>1 in all the experiments discussed above, and fluid motion is controlled by buoyancy, thus ensuring large-scale circulation in the crystal growth chamber. Rotation plays an important role locally in equalizing solutal concentrations and maintaining stable growth conditions.

The directional nature of gravity imparts certain peculiar properties to the buoyancy field. Specifically, the strength of convection patterns over the horizontal faces of the crystal depends on whether the face is aligned or opposed to the gravity vector. The downward facing surface is stabilized by gravity, experiences weak convection and has the smallest concentration gradients (as seen in Figure 5.22(a)) (Lecture 31). At a later point of time, convection in the bulk of the solution drives fluid flow over the lower surface as well, thus increasing the concentration gradients. A second consequence of weak convection is that the influence of rotation is felt strongly even at small time leading to a rapid increase in concentration gradients. This result is once again to be observed in Figure 5.22(a) (Lecture 31).

Previous Next

CONVECTION AROUND A GROWING KDP CRYSTAL

Imaging of three dimensional convection patterns around the growing KDP crystal is discussed here. Four view angles are considered for tomographic reconstruction of the concentration field. In the experiments conducted, the crystal is not disturbed during the recording of the projection data. In addition, longer durations of crystal growth have been considered. Since finite time is required to turn the beaker and record projections, experiments have been conducted when the concentration field around the crystal is nominally steady. Occasionally, the plume above the crystal is marginally unsteady, and a time-averaged sequence of schlieren images has been used for analysis. The increment in the view angles is 45^{o}, covering the range of 0 to 180^{o}.

The crystal growth process has been initiated by inserting a spontaneously crystallized KDP seed into its supersaturated solution at an average temperature of 35^{o}. This step is followed by slow cooling of the aqueous solution. The cooling rate employed is 0.05^{o}C/hour. The seed thermally equilibrates with the solution in about 20 minutes. With the passage of time, the density differences within the solution are solely due to concentration differences. Adjacent to the crystal, the solute deposits on the crystal faces, and the solution goes from the supersaturated to the saturated state. When the crystal size is small, salt deposition from the solution on to the crystal occurs by gradient diffusion. Diffusive transport has been sustained for a longer duration of time (and larger crystal sizes as well) by maintaining a small degree of supersaturation in the solution.

Previous Next

TOMOGRAPHIC RECONSTRCUTION OF SCHLIEREN DATA

The question of a correlation between the solutal distribution in the solution and the topography of the crystal can be partially addressed by reconstructing the solute concentration contours on select planes above the crystal. Reconstruction from schlieren images using principles of tomography is discussed in the present section. Unlike the hanging crystal configuration in Sections Comparision of Interferometry, Schlieren and Shadowgraph in a crystal Growth Experiment and Influence of Ramp Rate and Crystal Rotation on Convection Patterns, the crystal in the set of experiments was mounted over a platform. With this arrangement, the interference of the rising convection plume with the crystal holder is eliminated. Recording projections requires the apparatus to be turned; in this respect, what is collected is time-lapsed data. For meaningful analysis, it is thus necessary that the convection pattern be steady in time. Only those experiments where this requirement was fulfilled have been included in the discussion.

One parameter that defines the quality of the growing crystal is the symmetry of its faces. Since growth from an aqueous solution is governed by the strength and movement of buoyancy-driven convection currents, the convective field plays an important role in transporting solute from the bulk of the solution to the crystal faces. Hence, to ensure symmetric growth of the crystal, it is necessary to ensure that the convective field in the growth chamber retains a symmetry pattern. In the present discussion, a viewpoint that an axisymmetric convective field is favorable for crystal growth has been adopted. Thus, conditions under which the solutal distribution is axisymmetric have been delineated from the tomographic reconstructions.

Results are presented for experiments on crystal growth in the diffusion as well as steady convection regimes. In Section CONVECTION AROUND A GROWING KDP CRYSTAL , results have been presented in the form of a time sequence of schlieren images recorded at four view angles, corresponding to four pairs of optical windows of the growth chamber. The crystal is not disturbed during the growth process. In this respect, the measurement process is truly non-invasive, though with a drawback of allowing only a limited number of projections. The emphasis is towards understanding the diffusion-dominated and the stable growth regimes of the crystal. In both regimes, the concentration field is practically steady, particularly during the recording of the individual projections. The reconstruction of the concentration field over selected planes above the crystal and their relationship to the crystal geometry are discussed. The influence of crystal rotation on the convective field is not covered in the present discussion.

Previous Next

GROWTH PATTERNS IN THE DIFFUSION REGIME

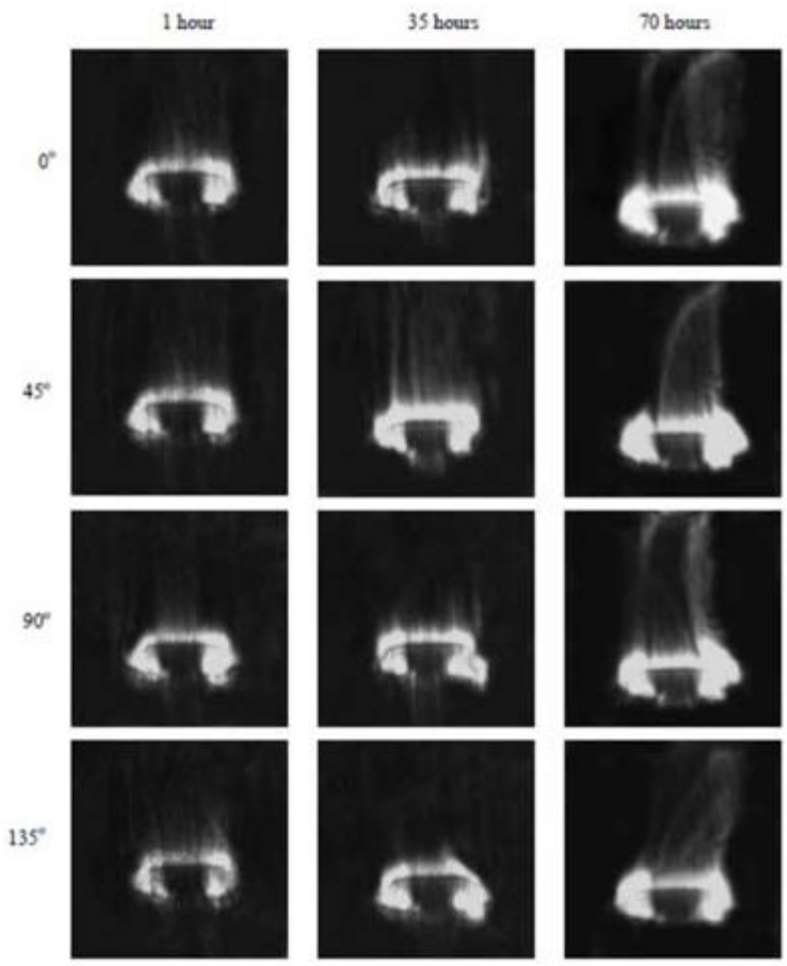

Figure 5.26: Schlieren images of the convective field around the crystal growing from its aqueous solution in a platform techniques at three different time instants recorded from the four view angles are presented.

Figure 5.26 shows schlieren images of a growing crystal in the diffusion-dominated regime at three different time instants. All four view angles are included in the figure. Adjacent to the crystal the deposition of solute from the solution to the crystal surfaces results in a change of concentration. This introduces a variation in density, refractive index and hence results in intensity contrast. For small time (less than one hour), intensity changes are restricted to the vicinity of the crystal. Here, transport of the solute to the crystal is purely by diffusion. At later times, a weak convection current is to be seen in the spread of light intensity above the crystal, though diffusion is still the dominant mechanism for solutal transport. For times greater than 70 hours, steady convection was seen to be clearly established in the form of a buoyant plume. In view of the small degree of supersaturation, the origin of convection here is related to an increase in the crystal size, rather than density differences.

Previous Next

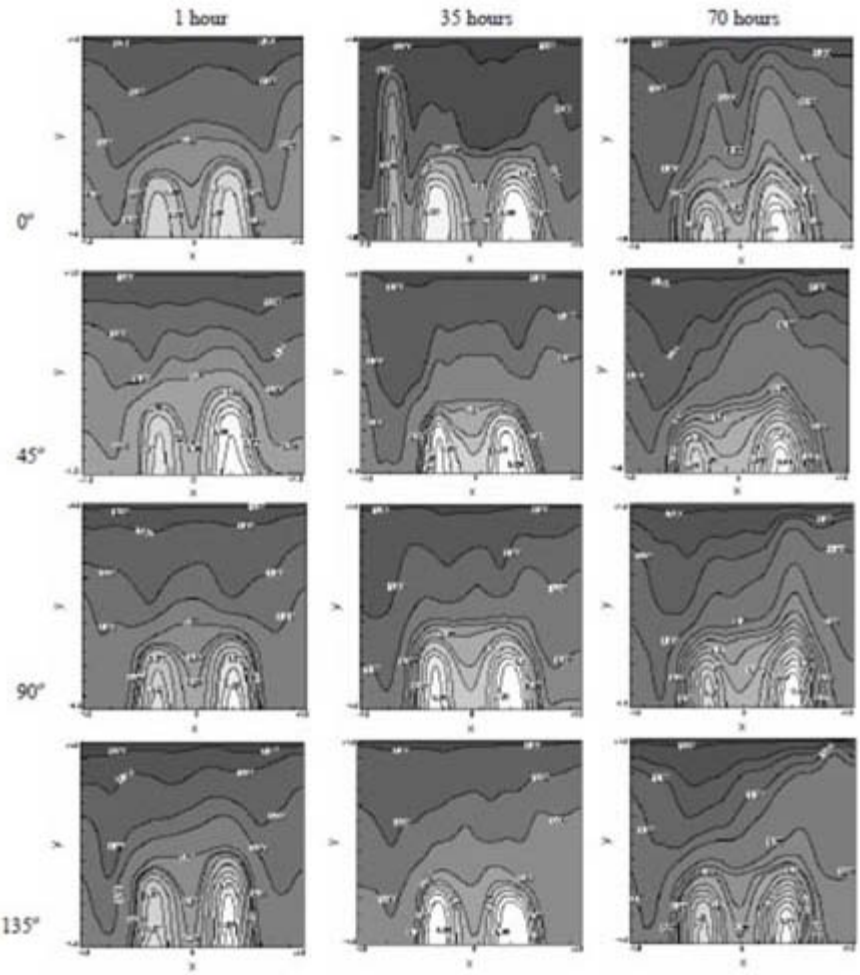

Figure 5.27: Concentration contours around a growing crystal at three different time instants in a diffusion dominated growth process for the four view angles.

Previous Next

Figure 5.27 shows normalized concentration maps above the growing crystal as derived from the schlieren images of Figure 5.26. The value of $C = 0$ represents a saturated solution, while the limit $C = 1$ refers to the supersaturated solution at its instantaneous temperature in the growth chamber. The maximum crystal size at the end of each experiment has been used to non-dimensionalize the *x* and *y* coordinates. For $t = 1$ hour, the concentration contours of Figure 5.27 in the bulk of the solution reveal an almost symmetric solute distribution. Symmetry can also be gauged by the identical nature of contour distributions for each view angle. The contours are not densely spaced, indicating low concentration gradients. The contours are localized in the vicinity of the crystal, with the bulk of the solution being at the supersaturated state $(C = 1)$. Hence this phase of the experiments corresponds to the growth process with transport across a diffusion boundary layer attached to the crystal. With the passage of time, the crystal size increases and the concentration gradients increase in strength. At this stage, the concentration field is accompanied by a partial loss of symmetry. Experiments of the present study revealed a marginal unsteadiness as well. This phase defines a transition process from diffusion-dominated transport of solute to the onset of convection. With the passage of time, a weak convection current is set up around the crystal. The images recorded at *t*=70 hours also show a greater loss of symmetry in the concentration contours and a denser spacing closer to the crystal are to be seen.

Figure 5.28 shows the variation of concentration with respect to the (vertical) *y*-coordinate in the crystal growth chamber. The concentration referred here is an average obtained in the viewing direction of the laser beam and across the image as well. For averaging the concentration values in the *x*-direction, namely normal to the light beam, 11 columns along the width were selected. The concentration profiles for *t*=1 hour (Figure 5.28(a)) overlap in the bulk of the solution above the crystal for all the four view angles, thus revealing a uniform distribution of solute concentration in this region. At *t*=35 hours (Figure 5.28(b)), the differences in the profiles are quite noticeable. These differences can be attributed to the temporary unsteadiness that sets in when a transition from diffusion-dominated growth takes place towards convection. With the passage of time, the profiles become increasingly symmetric and overlap with each other. The growth now takes place in the presence of an upward rising convective plume (Figure 5.28(c)). The symmetry in concentration distribution indicates an almost uniform and symmetric deposition of solute onto the crystal surfaces. It is to be noticed that for the three time instants, the profiles show differences in the vicinity of the crystal $(y/H = 0.0)$. The morphology of the KDP crystal is pyramidal, as shown in Figure 5.29 in a photograph of a grown KDP crystal in the diffusion-dominated regime, at the end of 70 hours. The differences in the average concentration near the crystal can be traced to the non-symmetric shape of the crystal as well as large gradients at the crystal edges.

Previous Next

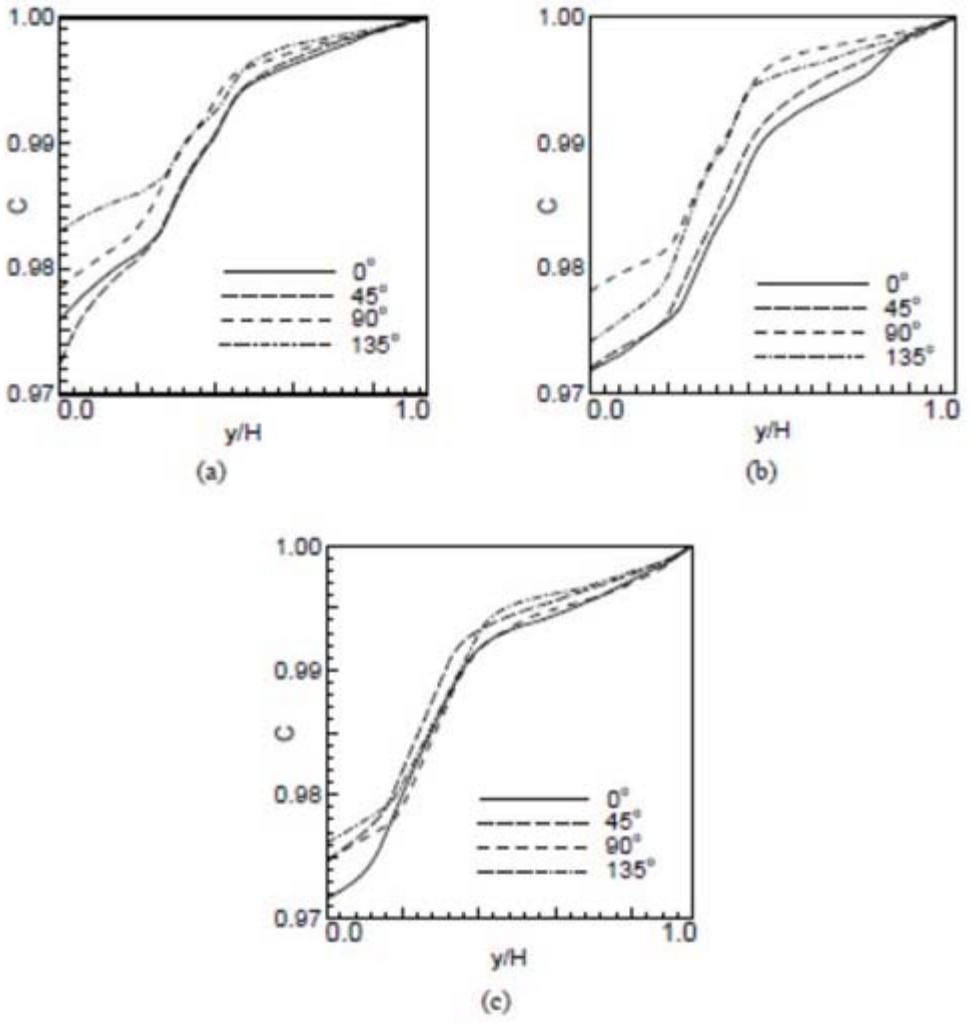

Figure 5.28: Width-averaged concentration profile as a function of vertical coordinate for the diffusion-dominant crystal growth. Time elapsed (a) 1 hour, (b) 35 hours and (c) 70 hours

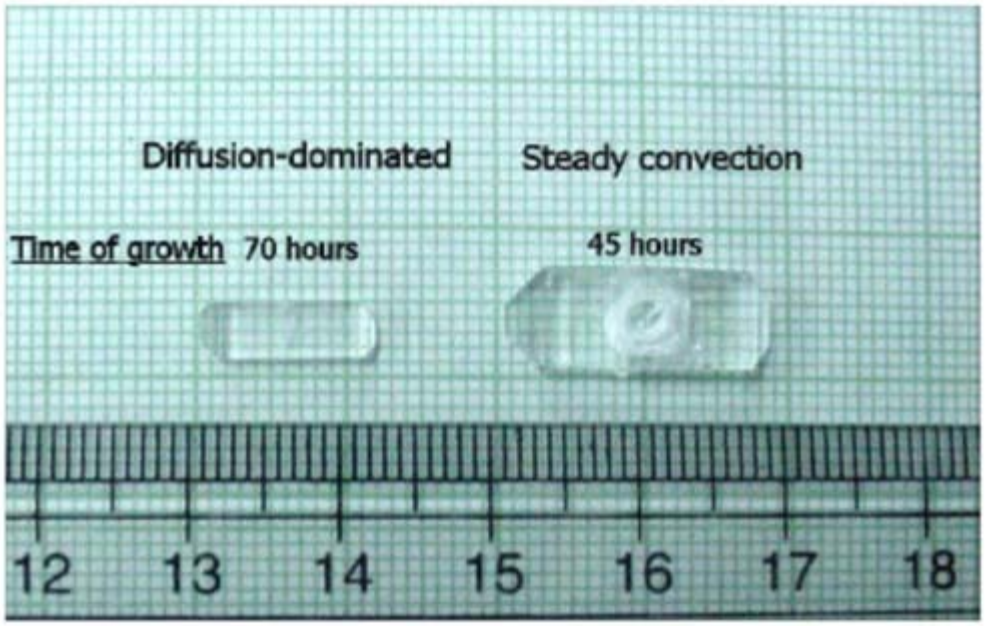

Figure 5.29: Photographs of as grown KDP crystals in diffusion-dominated (after 70 hours) and stable convection growth regimes (after 45 hours)

Previous Next

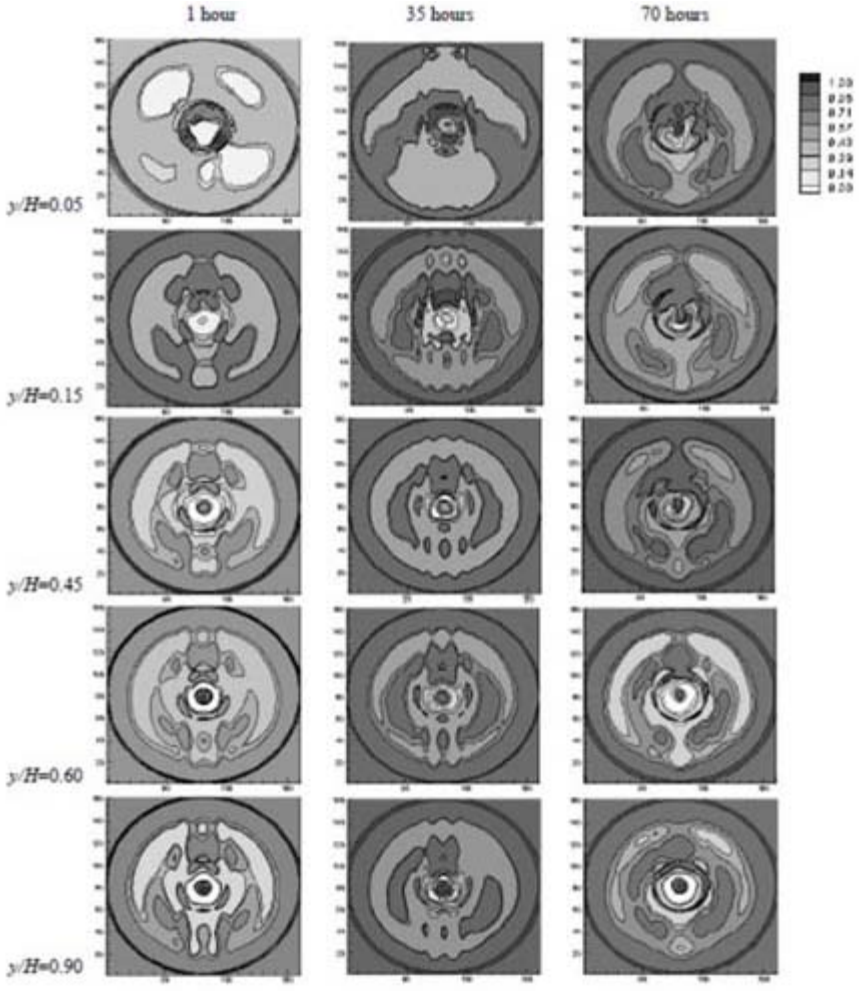

Figure 5.30: Reconstructed concentration profiles in the diffusion-dominated regime over five horizontal planes covering the range y/H=0.05-0.90, H being the vertical extent of the recorded schlieren image above the growing crystal.

Previous Next

Figure 5.30 shows the concentration profiles reconstructed over five horizontal planes $(y/H = 0.05, 0.15, 0.45, 0.60\ and\ 0.90)$ above the growing crystal. The location is just above the crystal while *y/H* = 0.90 represents a plane close to the top of the recorded schlieren image. The reconstructions correspond to the images presented in Figure 5.26. The outer circle represents the periphery of the beaker in which the crystal growth process is conducted. For a given time instant the images become progressively darker away from the crystal revealing the presence of supersaturated solution in the far field. At later times, as well as away from the crystal, the solution closer to the walls of the beaker is seen to be supersaturated, and the field is close to axisymmetric since the concentration contours here are circular. There is a significant departure from axisymmetry in the initial phase of crystal growth, as well as for longer times near the crystal itself. The second factor is explained by the fact that the crystal itself has a pyramidal structure and lacks circular symmetry. In the initial stages of growth, solutal transport is dictated by molecular diffusion from the solution to the crystal surface. Consequently, the lack of symmetry in the crystal morphology is felt on planes away from the crystal itself. At later times, a weak convection plume introduces the symmetry pattern of the beaker in the solute distribution. Hence, a degree of regularity is seen in the concentration contours, particularly on planes away from the crystal.

There are several interesting features to be noticed in Figure 5.30.

1. At the central core of the reconstructed cross-section, the dark shade indicates the presence of a supersaturated solution. The surrounding region is bright, indicative of solution depleted of salt. Thus, the deposition of the salt on the crystal is seen to occur on the periphery of the crystal. This is a region of bright light intensity (Figure 5.26) and hence high concentration gradients. The relationship between high gradients and preferential growth rates of the crystal faces is brought out in Section Influence of Ramp Rate and Crystal Rotation on Convection Patterns.
2. The concentration contours near the crystal $(y/H = 0.05\ and\ 0.15)$ show significant departure from symmetry during the initial stages of the growth process as well as during the transition phase $(t = 35\ hours)$. The transition referred here is the appearance of a convection plume that is gradually set up around the crystal, resulting in the partial unsteadiness in fluid motion. The loss of symmetry in the reconstruction can be traced to the unsteadiness as well. Symmetry is partly restored on planes above $y/H = 0.45\ at\ t = 35\ hours$ hours, indicating the influence of uniform solute concentration in the bulk of the solution. For *t*=70 hours, the convection plume is steady and the reconstructions are better structured closer to the crystal as well (for example, $y/H = 0.15$).
3. The spacing of contours in the central region is smaller for the convection regime, when compared to diffusion. Thus, convection increases the concentration gradients near the crystal, increases the salt deposition rate and hence the overall increase in crystal size (Figure 5.29). This is possibly the most suitable transport regime for crystal growth.

Previous Next

GROWTH PATTERNS IN THE CONVECTION REGIME

Crystal growth from a solution in which the limit of supersaturation has been reached is now considered. The density differences (ramp rate of 0.05°C/hour) as well as the crystal size (6 mm) are jointly large enough to sustain fluid motion in the beaker from the start. Experiments have been conducted under conditions of a steady plume rising from the crystal. Results for 30 hours of growth have been presented. For times greater than 30 hours, the plume became quite unsteady. Consequently, the projection data of individual view angles became uncorrelated.

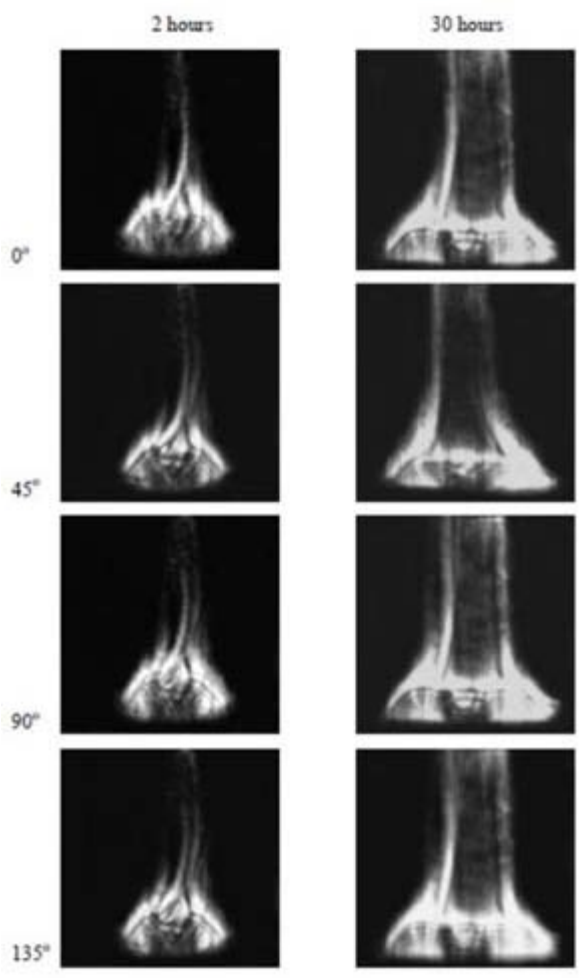

Figure 5.31: Schlieren images of the convective field around crystal growing from its aqueous solution as recorded from four different view angles at two different times instants (2 and 30 hours).

Figure 5.31 shows the convective field in the form of schlieren images. A well-defined plume rising from the top surface of the crystal is seen at both times of *t*=2 and 30 hours for four view angles. At *t*=2 hours, the plume was temporally stable, though a swaying movement was seen from one projection angle to the other. The swaying motion was due to the disturbance of the flow field caused by the turning of the growth chamber for recording the projection data. The tilt in the plume at selected angles for small time is also related to the non-symmetric shape of the initial crystal itself. At a later time (*t*=30 hours), the gradients are large enough to give rise to a stable and symmetric convective field. This is accompanied by uniform deposition of the solute on the crystal surfaces. As discussed in Section Growth Patterns in The Diffusion Regime, this regime yields the highest quality of the crystal in terms of symmetry of the faces and its transparency, along with the fastest growth rate.

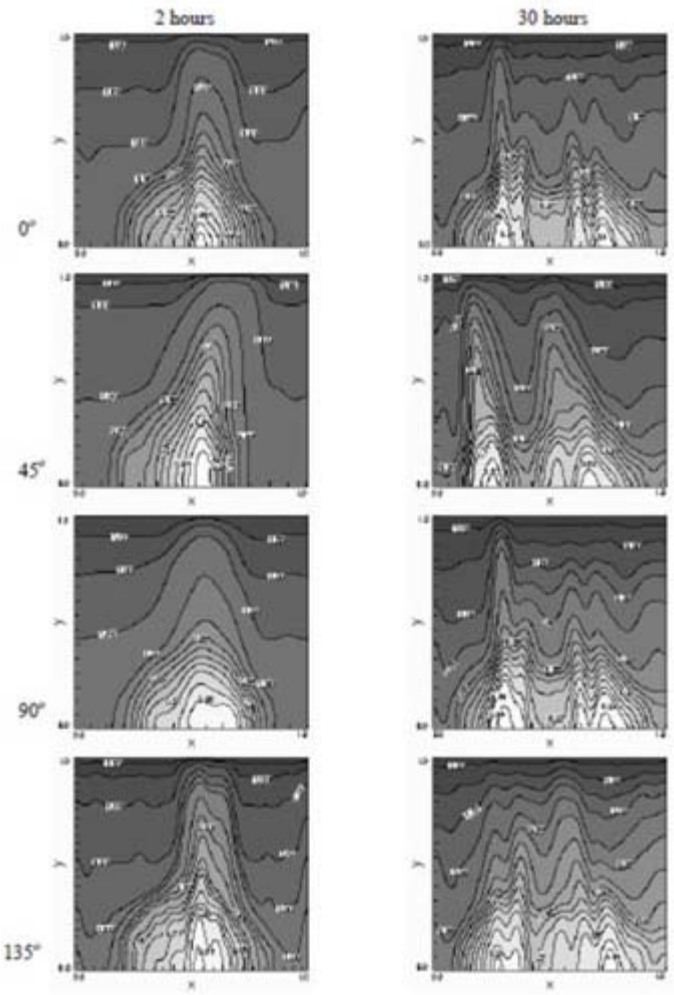

Figure 5.32: Concentration contours around a growing crystal in the presence of well-defined convective plume for the four view angles at two different time instants

Figure 5.32 shows concentration contours around the growing crystal derived from the schlieren images of Figure 5.31. The physical extent of the convective plume in the vertical direction can be estimated by the deformation of the concentration contours. Densely placed contours in the crystal vicinity are due to high concentration gradients. The contours at *t*=30 hours are seen to spread into the growth chamber, indicating that solute from the bulk of the solution itself is deposited over the crystal. The appearance of double peaks in the contour shape at the end of 30 hours confirms that the highest gradients and hence the deposition rates occur towards the edges of the crystal.

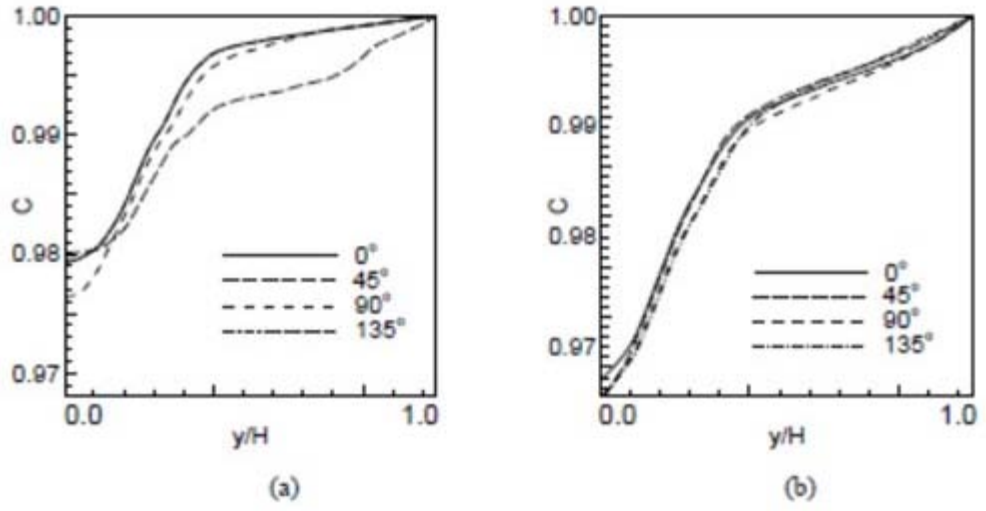

Figure 5.33: Width-averaged concentration profile as a functionn of the vertical coodinate around a growing crystal in the stable convection regime after a period of (a) 2 hours, and (b) 30 hours.

Figure 5.33 shows the distribution of width-averaged concentration with respect to the vertical coordinate at two time instants, namely 2 and 30 hours. The concentration data presented in the figure is integrated along the viewing direction by the light beam, and once again across the width of the image. The differences among the individual profiles for each of the view angles are a measure of loss of symmetry in the concentration distribution above the crystal. At *t*=2 hours, the differences are large in the bulk of the solution $(y/H \geq 0.55)$. The difference diminishes at locations closer to the crystal $(y/H = 0.0)$, Figure 5.33(a). With the passage of time, the convective plume stabilizes in terms of symmetry. The average concentration data corresponding to *t*=30 hours for the four view angles reveals a good degree of symmetry in the entire field of view above the crystal (Figure 5.33(b)).

Previous Next

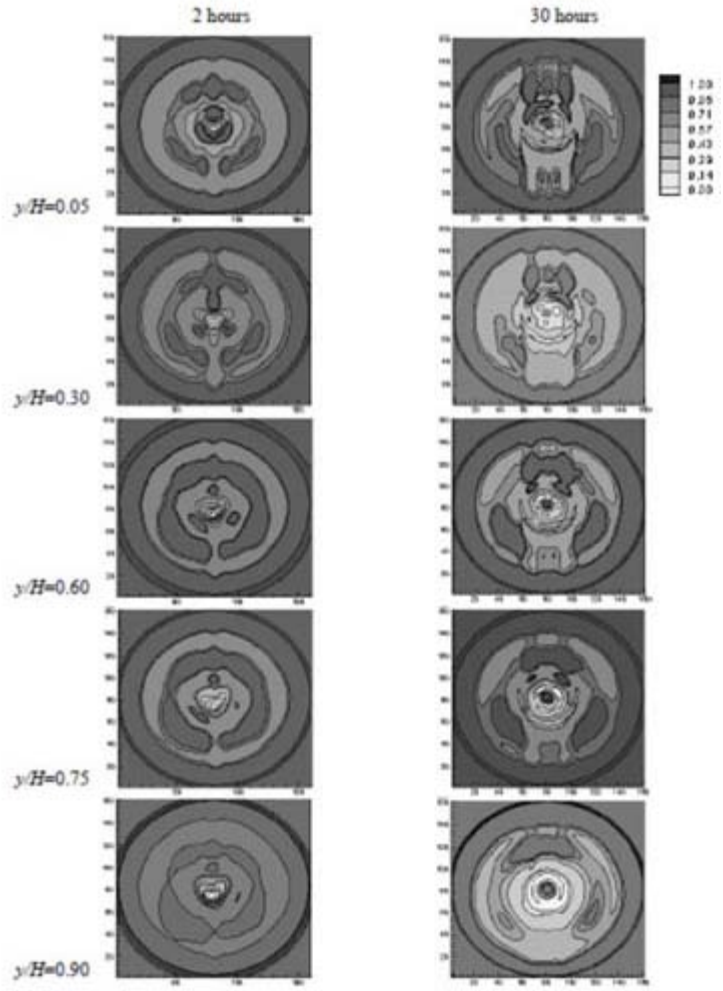

Figure 5.34: Reconstructed concentration profiles over five horizontal planes (y/H= 0.05-0.90) above the crystal growing in the presence of a stable convection plume. Time instants of 2 and 60 hours of experimental run time are presented.

Previous Next

Figure 5.34 shows reconstructed concentration profiles at selected horizontal planes above the growing crystal for the two time instants considered in Figure 5.31. The following observations can be recorded on the basis of the reconstruction.

1. At *t*=2 hours, the reconstructed concentration field reveals symmetry for the plane close to the crystal $(y/H = 0.05)$ both around the crystal and in the bulk of the solution. The presence of concentric rings indicates uniform distribution of concentration gradients on all the faces of the growing crystal. This feature is seen in Figure 5.31 as well, where the bright intensity region uniformly envelops the crystal faces. For planes away from the crystal $(y/H \geq 0.30)$, the deformation of the concentric rings in the vicinity of the crystal is mainly due to the swaying motion of the convective plume introduced by turning the growth chamber. This movement is also to be seen in the schlieren images of Figure 5.31. On the other hand, the bulk of the solution closer to the beaker shows uniform and symmetric distribution of concentration. The appearance of only a few contours in the solution shows low concentration gradients here in the initial stages of growth.
2. For all planes $(t = 2\ hours)$, the presence of a bright central core of the reconstructed cross-section is indicative of the solution depleted of salt. The spatial extent of the bright region at the center of the beaker is small, in agreement with the thin vertically rising buoyant plume above the growing crystal, Figure 5.31.
3. At later times $(t = 30)$, the concentration field at planes near the crystal $(y/H \leq 0.30)$ is not axisymmetric though the bulk of the solution near the boundaries of the growth chamber shows the presence of concentric rings. The loss of symmetry at the center of the reconstructed plane can be attributed to the role played by the crystal geometry in deciding the overall orientation of convection pattern. The effect of crystal shape is negligible when the size is small (for example, at *t*=2 hours) but is significant when the crystal grows in size with a well-defined morphology (Figure 5.29). In addition, densely spaced contours in the core and the bulk reflect the presence of high concentration gradients in the growth chamber.
4. For planes located away from the crystal $(y/H \geq 0.60)$, the effect of crystal geometry on the convective field is diminished. The presence of a dark central core (corresponding to a higher level of supersaturation) surrounded by a brighter region shows that high concentration gradients prevail on the crystal sides in comparison to its upper face.

Previous Next